


## Analytical Method to Estimate Railroad Spike Fastener Stress

Marcus S. Dersch<sup>1</sup>, Matheus Trizotto Silva<sup>1</sup>, J. Riley Edwards<sup>1</sup>, Arthur de O Lima<sup>1</sup>, and Tom Roadcap<sup>1</sup>

Transportation Research Record  
2020, Vol. 2674(11) 379–389  
© National Academy of Sciences:  
Transportation Research Board 2020  
Article reuse guidelines:  
sagepub.com/journals-permissions  
DOI: 10.1177/0361198120949259  
journals.sagepub.com/home/trr  


### Abstract

Previous research indicates that spike fastener fatigue failures have led to at least ten derailments since 2000. Given that railroads continue to install fastening systems that have experienced spike failures, methods to quantify the stress state of the spike must be developed. Common approaches to quantify the effect of key variables include laboratory experimentation, field instrumentation, or finite element model development. However, these approaches may be both time and cost prohibitive. An analytical method based on beam on elastic foundation mechanics, similar to the analysis of laterally loaded piles in deep foundation design, was developed to estimate the spike stresses. The outcome is a laboratory-validated analytical approach that generates estimates of spike stress. This analytical model was used to investigate key design criteria (timber modulus, spike cross-sectional area, and load applied) that could be changed to improve the resiliency of the fastening system to increase railroad safety. Another outcome of this study is the development of an instrumented spike that quantifies the spike demands when installed and loaded within a crosstie.

Improving safety within the rail industry is of first importance (*1*), with the industry having the goal of zero derailments. It has been found that at least ten derailments have occurred since the year 2000 because of wide track gauge resulting from broken spikes, many of which occurred within premium fastening systems (*2–4*). Railroad spikes are an element of track fastening systems that typically either hold the rail to a timber or composite crosstie, hold a steel load-distributing tie plate to the crosstie, or both. Cut-spikes typically have a square cross-section, and most fastening systems use two to four spikes per plate. Research thus far has indicated that excessive lateral (forces perpendicular to the length of the rail), longitudinal loads (forces parallel to the length of the rail), or both, have led to spike fatigue failures (*2, 5*). Research is needed to both understand the mechanics of these failures (*4, 6, 7*) and to develop tools which will provide a means to understand how various design solutions could mitigate the failures.

Multiple approaches could be pursued to quantify the magnitude and distribution of stress within the spikes when driven into a timber crosstie. Common methods within the rail industry to analyze and quantify the spike stress state or test new fastening system components consist of finite element models (FEMs) (*4, 8–11*), laboratory testing (*12*), or field-experimental programs (*13–17*).

Each of these methods is not without its cost in relation to both time and funding, especially full-scale field-testing programs. A limited number of design solutions can be tested in the laboratory, and fewer in the field within a reasonable timeframe. Consequently, a common approach is to develop FEMs to relatively quickly perform an analysis of the key variables affecting a given result. Despite their benefits, the development, execution, and validation of FEMs require special care and expertise, thus increasing an opportunity for inaccurate results (*18*).

To address the need to develop an accurate method to estimate the stress state of spikes driven in timber crossties, the Rail Transportation and Engineering Center (RailTEC) at the University of Illinois at Urbana-Champaign (Illinois) adapted an analytical solution based in mechanics. This solution, originally developed for analyzing laterally loaded driven piles for deep foundations, provides an opportunity to accurately analyze the stress of the spike. This approach was validated using

<sup>1</sup>Department of Civil and Environmental Engineering, Rail Transportation and Engineering Center – RailTEC, University of Illinois at Urbana-Champaign, Urbana, IL

### Corresponding Author:

Marcus S. Dersch, mdersch2@illinois.edu

laboratory experimental data and was used to provide insight into design approaches that could improve the resiliency of the spikes and increase the safety of rail infrastructure.

## Methodology

The analysis of laterally loaded driven piles is rooted in the mechanics of a beam on an elastic foundation as proposed by Winkler (19). The methodology proposed here follows a similar structure as presented by Long (20). Though not used in foundation design, Kerr (2003) (21) leverages these same mechanics' principles in his methods for analytically assessing the track structure and its response to load. Through the proposed analysis method, one can quantify the resulting displacement, shear, bending moment, and slope of a beam (pile or spike) subjected to lateral loading. Applying these to the case of a spike, the lateral loading represents a force from the train through the rail and tie plate and into the top of the spike. This analysis must consider that reaction (resistance) of the surrounding medium (soil or timber) is dependent on the beam's movement. In turn, the beam's movement is dependent on the surrounding medium response. One must consider this as an interaction problem between the beam and surrounding medium; in this case, the spike and timber. The following sections will first describe the development of equations for analyzing the spike behavior and then detail the equations for analyzing the timber's response.

The solution to the interaction problem of a spike which is loaded perpendicular to a given face (laterally or longitudinally) in timber described here follows the  $p$ - $y$  method that is commonly used by engineers around the world in quantifying the deflection of a laterally loaded pile in soil (22). For the purposes of this paper, and unless otherwise referenced, regardless of the global direction of the load application (lateral or longitudinal), the general loading case will be referenced as a laterally loaded spike. A visual representation of the interaction between the spike and timber used to develop the analytical solution is similar to the beam on elastic foundation proposed by Winkler (19) (Figure 1). The timber is continuous and a deformation at any point will cause a deformation at all other points. It is assumed, however, the interaction is a set of discrete, independent springs. The results in this paper will show this assumption to be sufficient for this analysis, as it is for piles driven into soil.

The resulting behavior of a laterally loaded spike can be solved using differential equations that are rooted in the relation between bending moments and curvature. The problem can be solved assuming the spike and timber remain in equilibrium and remain compatible via

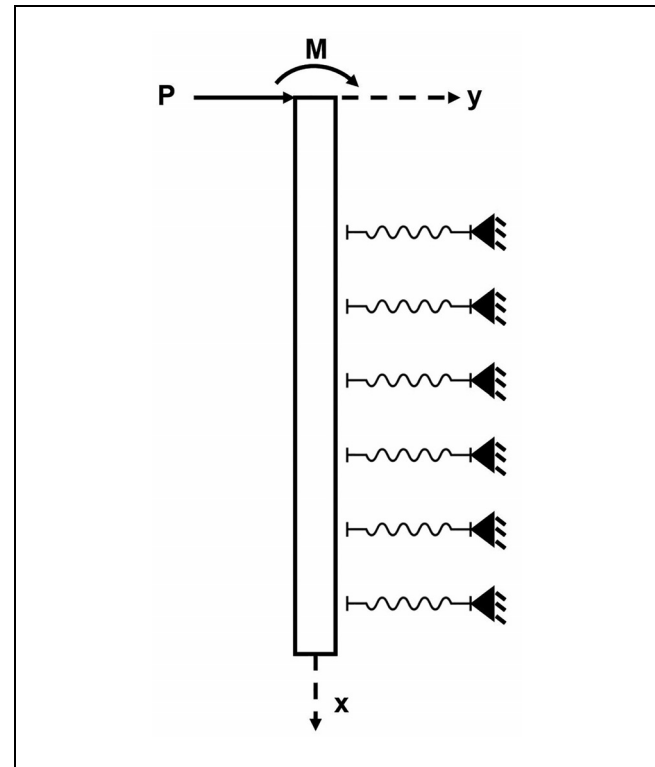


**Figure 1.** Visual representation of mathematical setup to model interaction of spike with surrounding timber medium when subjected to lateral loading from tie plate.

appropriate boundary condition assumptions. If all assumptions can be maintained, then a solution for the spike response can be developed along the entire length of the spike. If assumptions are not maintained (e.g., permanent deformation of the timber occurs, spike experiences yielding, etc.), then the closed form solution will no longer be applicable. Therefore, care must be taken when applying this analytical approach to various problems.

For this analysis, the following assumptions must be satisfied:

- The spike is straight and has a uniform cross-section
- The spike has a longitudinal plane of symmetry and loads and reactions lie in that plane
- The spike material is homogeneous
- The proportional limit of the spike material is not exceeded
- The modulus of elasticity of the spike is the same for tension and compression
- Transverse deflections of the spike are small
- The spike is not subjected to dynamic loads
- Deflections caused by shearing stresses are negligible

One must assume that plane sections remain plane as the spike is loaded and slope  $dy/dx$  is very small. With these

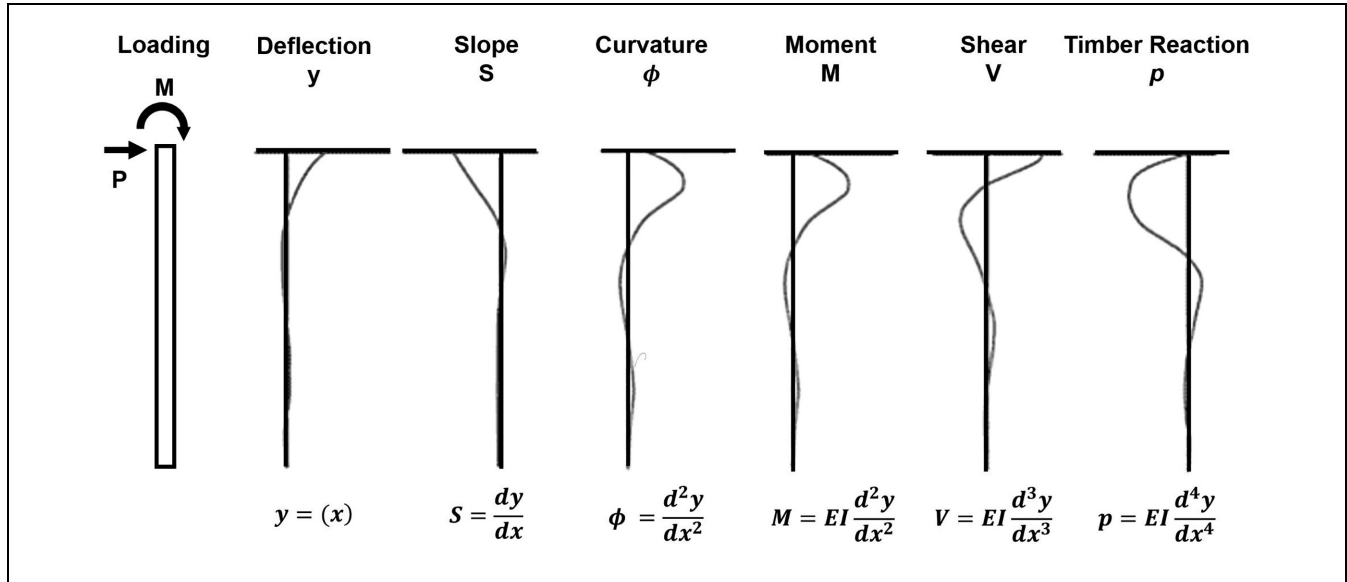


**Figure 2.** Visual representation of spike response to loading, with accompanying equations to calculate parameters.

assumptions in place, the relationship between moment,  $M$ , and curvature,  $\phi$ , (Equation 1) is applied and an expression for  $\phi$  in relation to  $x$  and  $y$  (Equation 2) is obtained where the  $x$ -axis is lying along the axis of the unloaded spike and the  $y$ -axis is the lateral deflection of the spike.

$$\phi = \frac{M}{EI} \quad (1)$$

$$\phi = \frac{d^2y}{dx^2} \quad (2)$$

When combining Equations 1 and 2, we arrive at the desired differential equation considering the moment,  $M$ , (Equation 3) and further equations for shear,  $V$ , (Equation 4) and timber reaction,  $p$ , (Equation 5) can be developed.

$$\frac{M}{EI} = \frac{d^2y}{dx^2} \quad (3)$$

$$\frac{V}{EI} = \frac{d^3y}{dx^3} \quad (4)$$

$$\frac{p}{EI} = \frac{d^4y}{dx^4} \quad (5)$$

Figure 2 provides a visual summary of a spike's response to lateral load using a full analysis considering a simply supported beam with uniform loading. For a full derivation of these equations, see Hetényi (23).

Understanding the timber's response is critical to developing an accurate method to analyze the spike response. As mentioned previously, the timber response

is characterized as a set of discrete mechanisms as suggested by Winkler (19). Figure 3 provides a visualization of one of these discrete mechanisms. Figure 3a is a view of the spike after installation. The stress distribution against the spike is shown in Figure 3b before any lateral load is applied. After a lateral load is applied, the stress distribution is altered and is represented by Figure 3c. Integration of the stress distribution shown in Figure 3c produces a force per unit length along the spike ( $p$ ).  $p$  is defined as the soil reaction and acts in the opposite direction to any spike deflection,  $y$ ; therefore the resulting naming convention of  $p$ - $y$  curves.

To apply these methods, there must be no shear stress at the surface of the spike parallel to the  $y$ -axis and lateral resistance and moment at the base of the spike can be accounted for by a  $p$ - $y$  curve at the side of the spike near the timber cross-tie surface. Further, there is no adjustment made for the effects of the spike installation, given it is assumed that the effects of spike installation are principally confined to an area close to the spike whereas the timber to react against the spike is several spike diameters greater in size. Errors caused by these assumptions are considered minimal and reasonable, given Dersch et al. (4) notes that some spikes can be pulled out by hand, thus indicating the reaction from installation is not permanent.

Timber response could perhaps be obtained from theory, though many more assumptions would need to be made. Further, the timber response could also be directly measured via load cells in the timber or similar instrumentation methods. However, the authors did not believe either of these approaches would produce accurate results and therefore quantified the timber response from

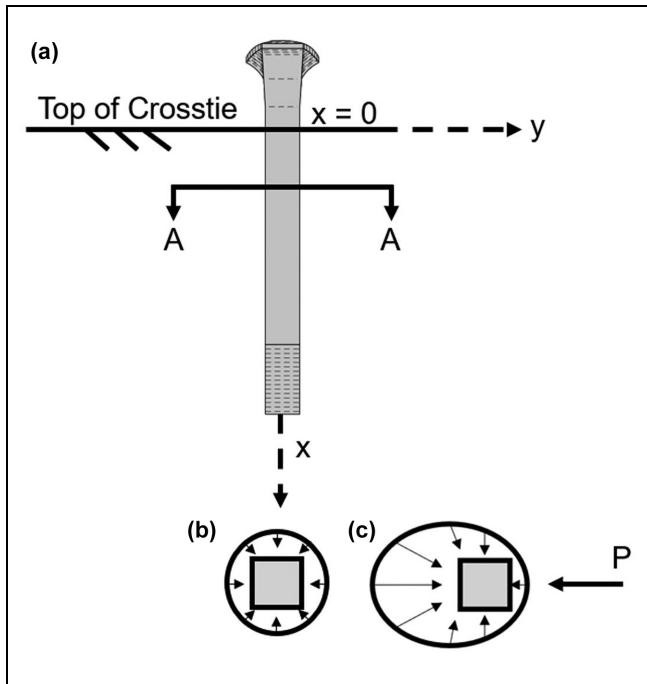


**Figure 3.** View of a spike after installation (a) with representations of forces on the spike in the unloaded condition, (b) and the condition with a lateral or longitudinal load (c).

experimental moment curves. This method is consistent with methods from geotechnical engineering in the development of soil p-y curves.

Experimental moment curves were created using data recorded by strain gauges installed on spikes driven into timber crossties and loaded laterally. Timber is anisotropic (24), making direction of the loading a critical parameter. The lateral load was applied perpendicular to timber grains, given this would be more detrimental than if the load was applied parallel to the grain (4) because the timber is weaker in this direction (24).

The computation of the timber's reaction along the length of the spike involves two differentiations of a bending moment curve. Matlock (25) performed this differentiation numerically for piles driven in soil with accurate measurements. p-y curves can then be plotted when multiple curves representing the distribution of deflection and soil reaction are acquired.

With the differential equations developed and the timber's reaction understood, the full derivation of the solution to the differential equations listed previously can be completed. The solution can consider the spike as an "infinite" or "finite" beam. In either case, the assumptions made were: the spike is assumed to be supported along its entire length; the timber's reaction, p, per unit length of spike is related to the deflection, y, by the timber modulus,  $E_t$ ; timber modulus is assumed to be

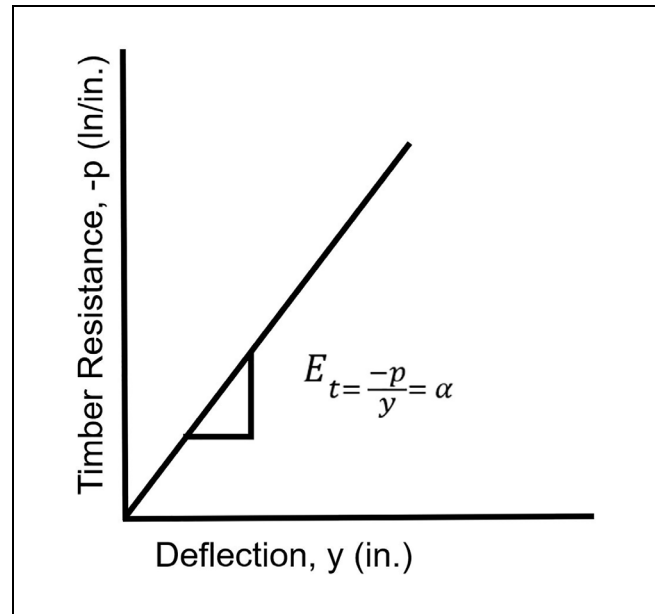


**Figure 4.** Constant timber modulus results from relationship between timber's reaction and deflection and constant, uniform cross-section assumptions.

uniform (Figure 4); and the spike modulus, E, and cross-section are consistent.

Considering the relationship between the timber reaction, p, and spike deflection, y, and using basic identities, Equation 6 was derived.

$$\frac{d^4y}{dx^4} + 4\beta^4y = 0 \tag{6}$$

Manipulation of Equation 6, while employing Equations 3–5, produces the basic differential equations for slope, moment, shear, and timber reaction as established in Equations 7–10.

$$\frac{dy}{dx} = \beta e^{\beta x} (\overline{C}_1 \cos(\beta x) + \overline{C}_2 \sin(\beta x) - \overline{C}_1 \sin(\beta x) + \overline{C}_2 \cos(\beta x)) + \beta e^{-\beta x} (-\overline{C}_3 \cos(\beta x) - \overline{C}_4 \sin(\beta x) - \overline{C}_3 \sin(\beta x) + \overline{C}_4 \cos(\beta x)) \tag{7}$$

$$\frac{d^2y}{dx^2} = 2\beta^2 e^{\beta x} (\overline{C}_2 \cos(\beta x) - \overline{C}_1 \sin(\beta x)) + 2\beta^2 e^{-\beta x} (\overline{C}_3 \sin(\beta x) - \overline{C}_4 \cos(\beta x)) \tag{8}$$

$$\frac{d^3y}{dx^3} = 2\beta^3 e^{\beta x} (\overline{C}_2 \cos(\beta x) - \overline{C}_1 \sin(\beta x) - \overline{C}_2 \sin(\beta x) - \overline{C}_1 \cos(\beta x)) + 2\beta^3 e^{-\beta x} (-\overline{C}_3 \sin(\beta x) + \overline{C}_4 \cos(\beta x) + \overline{C}_3 \cos(\beta x) + \overline{C}_4 \sin(\beta x)) \tag{9}$$

$$\frac{d^4y}{dx^4} = 4\beta^4 e^{\beta x} (-\overline{C}_2 \sin(\beta x) - \overline{C}_1 \cos(\beta x)) + 4\beta^4 e^{-\beta x} (-\overline{C}_3 \cos(\beta x) - \overline{C}_4 \sin(\beta x)) \tag{10}$$

where

$C_1, C_2, C_3, C_4$  are the coefficients to be evaluated at the given boundary conditions

To solve for these coefficients, the spike must be classified as finite or infinite, relative to the timber. For the spike to be considered infinite in length the relationship within Equation 10 must be satisfied, which requires Equations 11 and 12.

$$\beta L \geq 4 \tag{11}$$

$$\beta = \sqrt[4]{\frac{\alpha}{4EI}} \tag{12}$$

where

- $\beta$ , the relative stiffness factor
- $L$ , length of spike within the timber crosstie
- $E$ , elastic modulus of the spike
- $I$ , area moment of inertia of the spike
- $\alpha$ , modulus of the timber,  $E_t$ ,

Rearranging these equations results in Equation 13 which quantifies the timber modulus,  $E_t$ , threshold determining what spike embedment length,  $L$ , would be infinite or finite. This is possible when assuming the spike modulus,  $E$ , cross-section and length of the spike driven into the crosstie are constant—dependent on spike position (hold-down versus line).

$$E_t \geq \left(\frac{4}{L}\right)^4 \times 4EI; \text{ infinite} \tag{13}$$

For a 6.0 in. (152.4 mm) spike (26),  $L$  will approximately be either 5.00 in. (127.0 mm) for hold-down spikes or 4.20 in. (106.7 mm) for line spikes. Given  $E$  for the spike is assumed to be 29,000 kips per square inch (ksi) (200 GPa) and  $I$  is approximately 0.0127 in.<sup>4</sup> (5,300 mm<sup>4</sup>) for a standard 0.625 × 0.625 in. (15.9 × 15.9 mm) spike, the timber modulus must be greater than or equal to approximately 604 ksi (4.16 GPa) for hold-down spikes and approximately 1,213 ksi (8.36 GPa) for line spikes to be infinite. As Green et al. (24) indicate the modulus of timber perpendicular to grain ranges from 50 to 250 ksi (0.345–1.72 GPa) and timber parallel to grain ranges from 800 to 2,300 ksi (5.52–15.9 GPa), any standard 6 in. (152 mm) spike will be classified as finite when loading is applied perpendicular to the grain. If the spike length were increased such that the allowable timber modulus was reasonable (i.e., 7 in. [178 mm] spike), then an “infinite” analysis could likely be considered.

The key differences between the solutions between a finite and infinite beam are the assumptions that are made when preparing the solutions to the differential equations. Table 1 lists the boundary conditions for each condition.

**Table 1.** Governing Differential Equations and Boundary Conditions for Piles on Elastic Medium

	Boundary conditions	
	x = 0	x = L
Finite	$\frac{dy^2}{dx^2} = \frac{M}{EI}$ $\frac{dy^3}{dx^3} = \frac{P}{EI}$	$\frac{dy^2}{dx^2} = 0$ $\frac{dy^3}{dx^3} = 0$
Infinite	$\frac{dy^2}{dx^2} = \frac{M}{EI}$ $\frac{dy^3}{dx^3} = \frac{P}{EI}$	na  na

Note: na = not applicable.

With these boundary conditions, the coefficients of the differential equations listed previously for deflection, slope, moment, shear, and timber reaction can be determined for finite and infinite beams. The equations for infinite beams are straight forward and listed as Equations 14–18 below.

$$y = \frac{e^{-\beta x}}{2\beta^2 EI} \left[ \frac{P_t}{\beta} \cos(\beta x) + M_t(\cos(\beta x) - \sin(\beta x)) \right] \tag{14}$$

$$S = -e^{-\beta x} \left[ \frac{2P_t\beta^2}{E_s} (\cos(\beta x) + \sin(\beta x)) + \frac{M_t}{EI\beta} \cos(\beta x) \right] \tag{15}$$

$$M = e^{-\beta x} \left[ \frac{P_t}{\beta} \sin(\beta x) + M_t(\cos(\beta x) + \sin(\beta x)) \right] \tag{16}$$

$$V = e^{-\beta x} [P_t(\cos(\beta x) - \sin(\beta x)) - 2M_t\beta \sin(\beta x)] \tag{17}$$

$$p = 2\beta e^{-\beta x} [-P_t \cos(\beta x) - M_t\beta(\cos(\beta x) - \sin(\beta x))] \tag{18}$$

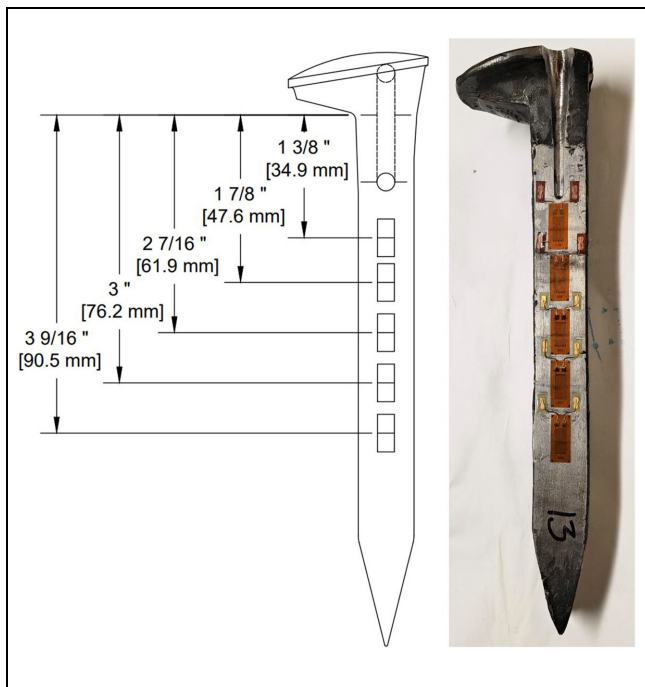
The equations for finite beams, unlike infinite beams, are non-trivial because the methods to solve for the coefficients is non-trivial. Table 2 shows all equations required to quantify the coefficients for finite beams.

### Validation

The results from this analytical solution were compared with data collected in the laboratory from a strain-gauged spike installed in timber that was laterally loaded perpendicular to the grain for validation. This was done to provide confidence in the approach and ensure the assumptions made would not restrict the usefulness of the model.

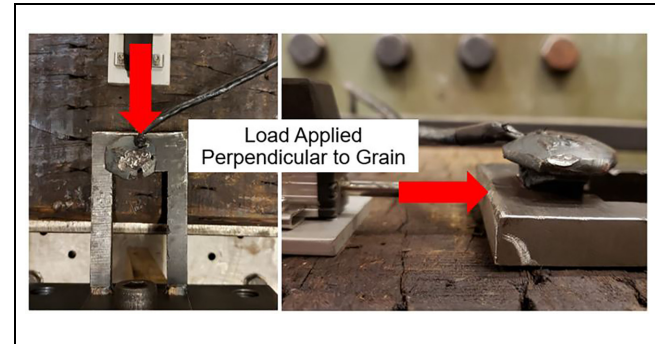
**Table 2.** Coefficients for Finite Beams

$C_1 = 2C_2 + C_3 - A_{15}$	$C_2 = \frac{A_{22}}{A_{20}} - \frac{A_{21}}{A_{20}} C_3$	$C_3 = \frac{A_{26}}{A_{27}}$	$C_4 = C_2 - A_1$
$A_1 = \frac{M_L}{2\beta^2 EI}$	$A_2 = \frac{V_L}{2\beta^2 EI}$	$A_3 = 2\beta^2 e^{\beta L} \cos(\beta L)$	$A_4 = 2\beta^2 e^{\beta L} \sin(\beta L)$
$A_5 = 2\beta^2 e^{-\beta L} \cos(\beta L)$	$A_6 = 2\beta^2 e^{-\beta L} \sin(\beta L)$	$A_7 = \beta A_3$	$A_8 = \beta A_4$
$A_9 = \beta A_5$	$A_{10} = \beta A_6$	$A_{11} = A_7 + A_8$	$A_{12} = A_7 - A_8$
$A_{13} = A_9 - A_{10}$	$A_{14} = A_9 - A_{10}$	$A_{15} = A_1 + A_2$	$A_{16} = A_3 - A_5$
$A_{17} = A_1 A_5$	$A_{18} = A_{12} + A_{14}$	$A_{19} = A_1 A_{14}$	$A_{20} = A_{16} - 2A_4$
$A_{21} = A_6 - A_4$	$A_{22} = A_{17} - A_4 A_{15}$	$A_{23} = A_{13} - 2A_{11}$	$A_{24} = A_{13} - A_{11}$
$A_{25} = A_{19} - A_{11} A_{15}$	$A_{26} = A_{25} - \frac{A_{22} A_{23}}{A_{20}}$	$A_{27} = A_{24} - \frac{A_{21} A_{23}}{A_{20}}$	

**Figure 5.** Plan and photo of instrumented spike for strain measurements.

The novel instrumented spike developed for this investigation consisted of five strain gauges as shown in Figure 5. Unlike previous instrumentation methods (6) which removed material from the spike, thus changing the behavior of the system, the strain gauges were placed directly on the prepared surface of the spike. Epoxy was used to protect the wires and strain gauges during installation and loading.

The instrumented spike was installed (i.e., driven) in a timber crosstie. The crosstie was installed in the loading frame and restrained from moving. A 1,500 lb (6.67 kN) load was applied perpendicular to the grain of the timber crosstie via a hydraulic actuator. This load magnitude was considered reasonable once the following was considered. First, AREMA recommends that a fastening system withstand at least a 2400 lb (10.7 kN) longitudinal load before rail slip for a single fastening system (or rail

**Figure 6.** Laboratory experimental setup for spike strain measurements.

seat) (12). Further, recent research has shown that the rail seat load is distributed within the spikes, with a single spike taking approximately 60% of the longitudinal load (27). Therefore, given that 60% of 2,400 is 1,440, this load magnitude was acceptable. Figure 6 shows how the loads were applied through a fixture providing a representative contact area of a tie plate. The strains were transformed into moments by rearranging Equations 19 and 20 and combining them into Equation 21. Further, it was assumed that the moments at  $x = -0.50$  in. ( $-12.7$  mm) and  $x = 5.0$  in. (127 mm) were 0, thus providing seven locations along the spike where the moment was known.

$$\sigma = \frac{My}{I} \quad (19)$$

$$\varepsilon = \frac{\sigma}{E} \quad (20)$$

$$M = \frac{\varepsilon EI}{y} \quad (21)$$

Moments at each location along the spike were plotted against the moments calculated via the analytical approach presented in this paper considering a finite spike for the load applied perpendicular to the grain. A 1,500 lb (6.67 kN) force was applied over an area of  $0.50$  in.<sup>2</sup> (322 mm<sup>2</sup>) in the analytical model which was

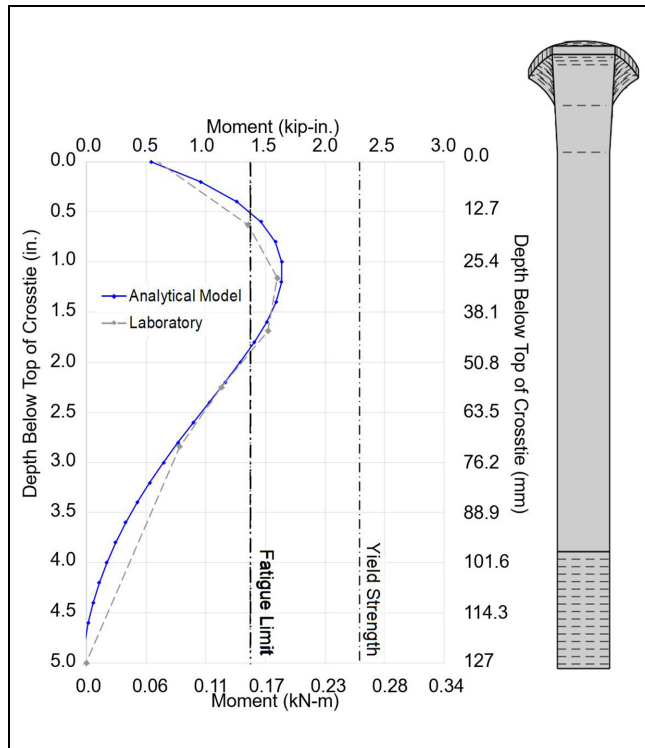


**Figure 7.** Comparison of laboratory-measured data with analytical model output.

representative of the loading fixture and is similar to the contact area of a tie plate for a hold-down spike. The modulus perpendicular to grain was assumed to be 200 ksi (1.38 GPa), which aligns with the value Dersch et al. (4) used in the validated FEM. Figure 7 shows the comparison of the results and also indicate the yield strength and fatigue limit moments. The results match well between  $x = 0.0$  and  $x = 3.0$  in. (76.2 mm) below the top of the crosstie. The difference between the analytical model and the laboratory results is near a minimum at a depth of 1.5 in. (38.1 mm). This is considered to be the most critical depth, as this is where failures are regularly found in the field (4). The moment values beyond 3.0 in. (76.2 mm) below the top of the crosstie do not match as well, but this is likely because of the assumption in relation to the location of zero moment for the laboratory condition. This is not considered to be as critical as it is not the area of maximum moment, nor is it the area where failures have been found in the field. The resulting moments also exceed the fatigue limit from approximately 0.5 to 1.9 in. (12.7–48.3 mm) below the top of the crosstie, which provides additional insight into why the spikes show variation in the depth of failure. Taken as a whole, this analytical approach provides an accurate means for analyzing the stress along the depth of the spike driven into timber crossties within a reasonable range of conditions and beyond load levels that would result in fatigue failures.

Key limitations of this analytical approach not accounted for include varying timber moduli with depth, changing modulus with load, and permanent plastic deformation within the timber. Therefore, care must be taken as to the cases which can be investigated, to avoid extrapolation of model results. Understanding these limitations, this analytical model can be used to help investigate a variety of case studies that involve varying key design parameters that can increase the strength of the track structure and increase track reliability.

## Case Studies

The literature suggests that the three factors that have the greatest effect on a p-y curve are the timber properties, spike geometry, and nature of loading (20). Therefore, this paper documents the effects of timber modulus, spike cross-sectional area, and load magnitude on the magnitude and locations of the maximum bending moment. All data are reported in relation to the fatigue limit and yield strength of the spike as reported by Dersch et al. (4).

### Effect of Timber Modulus

As this analytical approach cannot account for permanent deformation of the timber, the elastic modulus was the primary parameter studied. Further, given this analytical approach was validated at 1,500 lb (6.67 kN), this loading magnitude was held constant at each modulus value selected. Though there are limitations to the ability of railroads to procure specific crossties, the results from this study investigating modulus values of 100, 200, and 500 ksi (0.689, 1.38, and 3.45 GPa) (Figure 8). 100 ksi (.689 GPa) was chosen as a practical lower bound for the modulus of the timber perpendicular to the grain. 500 ksi (3.45 GPa) was selected as the upper bound for modulus of the timber as presented within this study because this was the level in which spike stresses fell below the fatigue limit. Further, this value aligns with the modulus of glass fiber-reinforced composite crossties (28), which could be used as a substitute for timber. Finally, though 500 ksi (3.45 GPa) is below the 800 ksi (5.52 GPa) lower bound for the modulus of timber parallel to grain, as mentioned previously, general trends can be found using this range.

The results indicate an inverse relationship between timber modulus and maximum spike stress in that, as timber modulus is decreased, the maximum moment in the spike increases. Although this appears to be inconsistent with observations in the field that have shown spikes in new crossties fail before older crossties (i.e., higher modulus crossties versus lower modulus), this result aligns with previous findings by Dersch et al. (4) that loading perpendicular to the grain is more detrimental



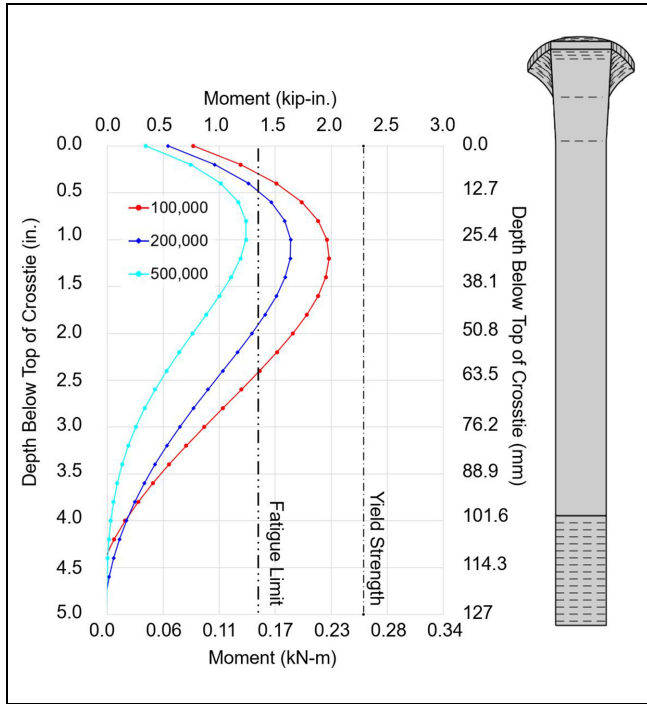


Figure 8. Dependency of moment on timber modulus.

than loading parallel to the grain, given the modulus and strength parallel to grain is greater. The authors hypothesize that the reason spikes fail more often in new crossies is because they are stiffer elements within the load transfer system and thus take a greater share of the applied load. Therefore, when there is a differential in tie stiffness, fastener loading demands on new, stiffer, crossies would be greater than older, less stiff, crossies. However, if all crossies exhibit an equal stiffness, as modulus decreases, the spike moment would increase.

Specifically, in this case, the moments for the 100 and 200 ksi (0.689 and 1.38 GPa) modulus cases both exceed the fatigue limit, indicating fatigue failures could occur if this load magnitude were experienced in the field regularly. The moment for the 500 ksi (1.38 GPa) case fell below the fatigue limit. As 500 ksi (1.38 GPa) produces moments below the fatigue limit, and lateral loads applied parallel to grain would be resisted by timber with modulus values greater than 800 ksi (5.52 GPa), fatigue failures would not be expected unless load magnitudes were greater in magnitude. This provides insight into the lack of spike failures in traditional fastening systems that do not utilize elastic fasteners.

Also, it can be seen that as the modulus is decreased the location of maximum moment, or failure, would become deeper in the crossie, moving from approximately 1.00 in. to 1.25 in. (25.4–31.8 mm) below the crossie surface. As a spike breaks deeper in a crossie, there is a greater likelihood it would become harder to

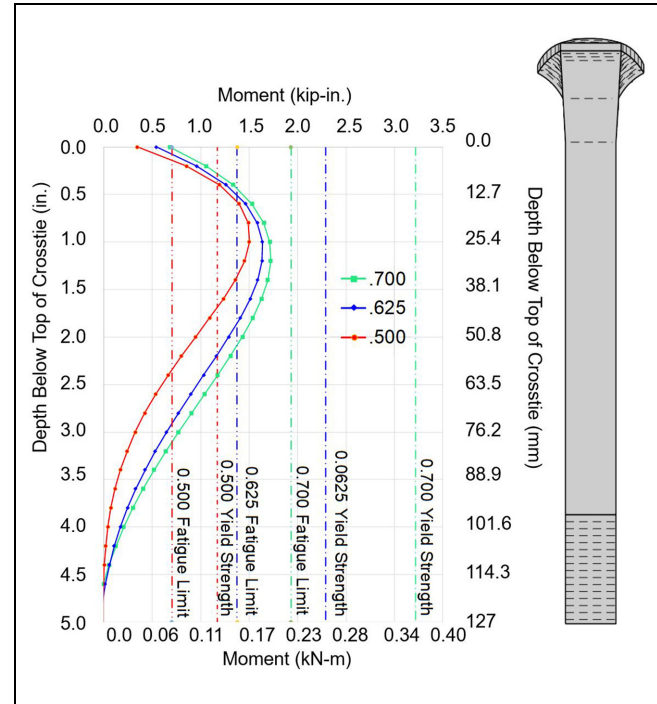


Figure 9. Dependency of moment on spike width, with associated moments required for steel fatigue and yield limits.

detect and a greater risk to the safety of railroad operations. Therefore, by specifying a crossie with a greater modulus, one is helping to ensure any failure could occur closer to the surface and be more easily identified during a track inspection.

### Effect of Spike Cross-Sectional Area

The next parametric study investigated the effect of spike geometry: specifically, while maintaining a square spike, a spike's width, which affects the cross-sectional area. As was the case for the previous study, the timber modulus was held constant at 200 ksi (1.38 GPa), as this was the value validated in the laboratory. This was studied given the spike geometry is likely the easiest parameter to change/control in the design of future fastening systems. A standard cut spike is 0.625 in. × 0.625 in. (15.9 × 15.9 mm), the smallest hole in a plate is 0.690 in. (17.5 mm), and the largest is 0.750 in. (19.1 mm). Therefore, to limit the requirement to change the spike hole size within every plate, while also attempting to limit the opportunity for tie splitting, square spikes with widths of 0.500, 0.625, and 0.700 in. (12.7, 15.9, and 17.8 mm) were investigated and the results are presented in Figure 9. Given the findings from the investigation into the effect of modulus and literature both indicate load applied perpendicular to grain is more detrimental



to the failure of spikes than parallel to grain, this loading direction was the only direction investigated.

As spike width is increased, the moment also increases from 1.5 kip-in. (0.169 kN-m) to 1.72 kip-in. (0.194 kN-m). This is attributed to the increased reaction from the timber as the width increases from 0.500 to 0.700 in. (12.7–17.8 mm). Though the moment increases, the capacity of the spike (fatigue limit and yielding strength) is increasing at a greater rate from 1.17 kip-in. to 1.93 kip-in. (0.132–0.218 kN-m) and 1.17 kip-in. to 3.22 kip-in. (0.132–0.364 kN-m), respectively. In the cases considered, the following “reserve” capacities (moment at yield/moment calculated at 1,500 lb [6.67 kN], load applied laterally perpendicular to grain) were found to be 0.8, 1.4, and 1.9 for 0.500 in., 0.625 in., and 0.700 in. (12.7, 15.9, and 17.8 mm) widths, respectively. Further, as the width is increased to 0.700 in. (17.8 mm), it is evident that the fatigue limit of the spike is no longer exceeded.

In addition, it should be noted that as width is increased, the depth to maximum moment is increased slightly. That is, as the width increased from 0.500 in. to 0.700 in. (12.7–17.8 mm), the depth increased from 1.0 in. to 1.2 in. (25.4–30.5 mm). This effect was less than timber modulus, and thus not considered as concerning given the safety factor is increasing as well. This indicates that one could consider increasing the spike width to increase the resiliency of these fastening systems and reduce the risk of spike failure.

### Effect of Load Magnitude

The last parametric study performed was an investigation into the effect of load magnitude, while holding timber modulus constant at 200 ksi (1.38 GPa), as this was the value validated in the laboratory. It is expected that as load was increased, the moment would also increase. However, this parameter was studied with the objective of providing further confidence in the performance of this analytical approach by comparing the results with published finite element analysis (FEA) results as well as understanding how the depth of maximum moment changes with load.

As expected, as the applied load was increased, the maximum moment also increased (Figure 10). The load at which the spike exceeds the yield stress is similar to what has been reported by the detailed FEA study by Dersch et al. (4), that is, between 2,000 and 3,000 lb (8.90 and 13.3 kN) applied perpendicular to grain, thus providing more confidence in the results from this analytical solution. The fatigue limit would be exceeded with a load magnitude between 1,000 and 1,500 pounds (4.45 and 6.65 kN), further indicating the sensitivity of spike stress to the loading perpendicular to the grain.

The depth to maximum stress also increased from 0.8 in. to 1.2 in. (20.3–30.5 mm), respectively. One comment

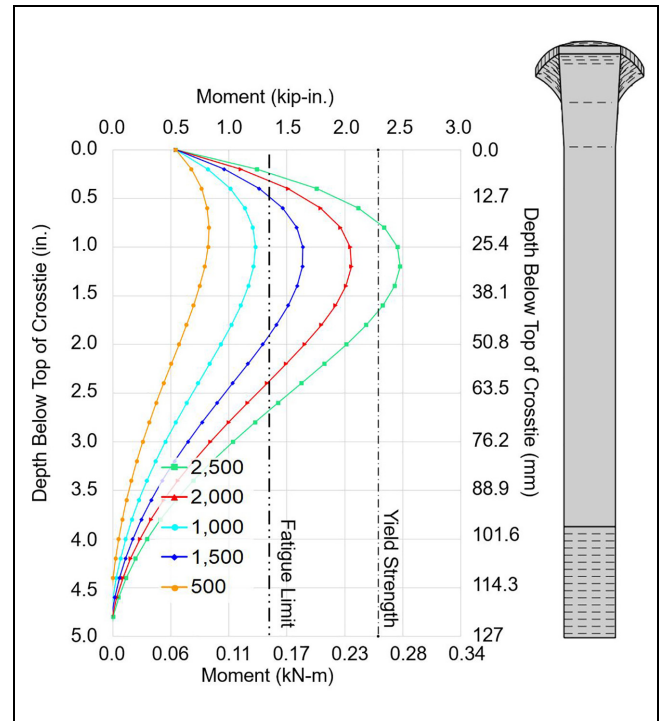


**Figure 10.** Dependency of moment on input force from the tie plate.

in relation to the shortcomings of this result is the depth to maximum moment is lower than would be expected based on the field failures and FEA results, which would have expected maximum moment to occur between 1.4 and 1.6 in. (35.6 and 40.6 mm) below the top of the crosstie. Therefore, although this model can estimate the demand on the spike within a reasonable range, the depth to maximum demand could be improved. The authors believe this is because this analytical model does not account for the timber behavior beyond its elastic limit.

### Conclusion

A laboratory-validated analytical method has been developed that accurately estimates the stress of spikes driven in timber crossties that relies on beam on elastic foundation mechanics and was adapted from methods used in deep foundation design. This analytical method was applied to multiple case studies quantifying the effect key variables have on spike stress. The results from these case studies demonstrate that the model can be used to improve fastener resiliency and increased railway safety through improved design recommendations. Further, though this study only investigated uni-directional loading, the findings can be generalized to account for bi-directional loading. That is, regardless of loading direction, a decrease in modulus, decrease in spike size, or

increase in load will lead to increased spike demands. Key findings from this research and the model generated are as follows:

- A validated analytical model has been developed and used to answer key design related questions that can lead to improved component and track resiliency
- An instrumented spike was developed that could survive installation and loading as well as quantify the spike demands during loading
- As timber modulus is increased (100–500 ksi) the:
  - Induced bending moments would be reduced (1.98–1.24 kip-in. [0.223–0.140 kN-m])
  - Depth to maximum stress would decrease (1.2–0.8 in. [30.5–20.2 mm])
  - Fatigue limit would no longer be exceeded above 500 ksi
- As spike width is increased (0.500–0.700 in. [12.7–17.8 mm]), the:
  - Factor of safety increases (0.8–1.9) at a greater rate than the induced bending moment (1.50–1.72 kip-in. [0.169–0.194 kN-m]), leading to increased resiliency
  - Fatigue limit would no longer be exceeded above 0.700 in. (17.8 mm) for this load case
  - Depth to maximum stress does not significantly increase (1.0–1.2 in. [25.4–30.5 mm])
- As loads applied perpendicular to the timber grain increase (500–2,500 lb), the:
  - Induced bending moments would increase (0.83–2.48 kip-in. [0.093–0.280 kN-m])
  - The depth to maximum stress also increases (0.8–1.2 in. [20.2–30.5 mm])

Therefore, to reduce spike stress and mitigate spike fatigue failures, and when feasible (economically, logistically, etc.) railroads could ensure the timber crossties installed with premium elastic fasteners in demanding locations had higher modulus values than other areas, could increase the size of spikes installed, or, mitigate the longitudinal and lateral loads applied through proven methods (top of rail lubrication, distributed power, etc.). Future work could include further model refinement and validation to provide greater applicability to a wider range of problems. In addition, this method will be used to execute additional case studies to further improve on the recommendations for improved spike resiliency.

### Acknowledgments

The authors would also like to formally thank Pouyan Asem and Niyazi Özgür Bezin for their encouragement and knowledge in relation to the laterally loading of piles in soil.

### Declaration of Conflicting Interests

The author(s) declared no potential conflicts of interest with respect to the research, authorship, and/or publication of this article.

### Funding

The author(s) disclosed receipt of the following financial support for the research, authorship, and/or publication of this article: This research effort is funded by the Federal Railroad Administration (FRA), part of the United States Department of Transportation (U.S. DOT). This work was also supported by the National University Rail Center, a U.S. Department of Transportation Office of the Assistant Secretary for Research and Technology Tier 1 University Transportation Center. The material in this paper represents the position of the authors and not necessarily that of sponsors. J. Riley Edwards has been supported in part by the grants to the UIUC Rail Transportation and Engineering Center (RailTEC) from CN and Hanson Professional Services.

### References

1. General Code of Operating Rules Committee. *General Code of Operating Rules*, 7th ed. General Code of Operating Rules Committee, 2015.
2. Roadcap, T., B. Kerchof, M. S. Dersch, M. Trizotto, and J. Riley Edwards. Field Experience and Academic Inquiry to Understand Mechanisms of Spike and Screw Failures in Railroad Fastening Systems. *Proc., AREMA Annual Conference with Railway Interchange*, American Railway Engineering and Maintenance-of-Way Association, Minneapolis, MN, 2019.
3. Stuart, C., T. Roadcap, and M. Dersch. *Timber Crosstie Spike Fastener Failure Investigation*. Research Results 19–14. Federal Railroad Administration, Office of Research and Development, 2019.
4. Dersch, M., T. Roadcap, J. R. Edwards, Y. Qian, J. Y. Kim, and M. Trizotto. Investigation into the Effect of Lateral and Longitudinal Loads on Railroad Spike Stress Magnitude and Location using Finite Element Analysis. *Engineering Failure Analysis*, Vol. 104, 2019, pp. 388–398.
5. Roadcap, T., M. Dersch, and J. R. Edwards. Load Environment and Force Transfer in Railway Fastening Systems: A Case Study of the Broken Spike Mystery. *Proc., 2019 World Congress on Railway Research*, Tokyo, Japan, 2019.
6. Dick, M. G., D. S. McConnell, and H. C. Iwand. Experimental Measurement and Finite Element Analysis of Screw Spike Fatigue Loads. *Proc., ASME/IEEE Joint Rail Conference and Internal Combustion Engine Division Spring Technical Conference*, Pueblo, CO, IEEE, New York, 2007, pp. 161–166.
7. Gao, Y., M. McHenry, and B. Kerchof. Investigation of Broken Cut Spikes on Elastic Fastener Tie Plates using an Integrated Simulation Method. *Proc., ASME/IEEE Joint Rail Conference*, Pittsburgh, PA, IEEE, New York, 2018.
8. Chen, Z., M. Shin, S. Wei, B. Andrawes, and D. A. Kuchma. Finite Element Modeling and Validation of the

- Fastening Systems and Concrete Sleepers Used in North America. *Proceedings of the Institution of Mechanical Engineers, Part F: Journal of Rail and Rapid Transit*, Vol. 228, No. 6, 2014, pp. 590–602.
9. Chen, Z., B. Andrawes, and J. R. Edwards. Finite Element Modelling and Field Validation of Prestressed Concrete Sleepers and Fastening Systems. *Structure and Infrastructure Engineering*, Vol. 12, No. 5, 2016, pp. 631–646.
  10. Chen, Z., and B. Andrawes. A Mechanistic Model of Lateral Rail Head Deflection Based on Fastening System Parameters. *Proceedings of the Institution of Mechanical Engineers, Part F: Journal of Rail and Rapid Transit*, Vol. 231, No. 9, 2017, pp. 999–1014.
  11. Edwards, J. R., L. Chavez, Y. Qian, A. de, and O. Lima. *Field Study and Analytical Modeling of the Performance of Existing WMATA Anchor Bolt System*. Final Report CQ17066. Washington Metropolitan Area Transit Authority, Washington, DC, 2018.
  12. American Railway Engineering and Maintenance-of-Way Association. AREMA - Chapter 30, Part 4: Concrete Ties. In *Manual for Railway Engineering*, The American Railway Engineering and Maintenance-of-Way Association, Lanham, MD, 2017.
  13. Akhtar, M. N., D. D. Davis, and J. A. LoPresti. *Improving Performance of Crossties and Fasteners*. TD-12-013. Association of American Railroads, Transportation Technology Center, Inc., Pueblo, CO, 2012.
  14. McHenry, M., and J. LoPresti. *Tie and Fastener System Gage Restraint Performance at FAST*. Technology Digest TD-15-013. Transportation Technology Center, Inc., Pueblo, CO, 2015.
  15. McHenry, M., and J. LoPresti. Field Evaluation of Sleeper and Fastener Designs for Freight Operations. *Proc., 11th World Congress on Railway Research*, Milan, Italy, 2016.
  16. Edwards, J. R., M. S. Dersch, and R. G. Kernes. *Improved Concrete Crosstie and Fastening Systems for US High Speed Passenger Rail and Joint Corridors: Volume 1 – Project Summary Report*. Technical Report DOT/FRA/ORD-17/23. U.S. Department of Transportation, Federal Railroad Administration, Washington, DC, 2017.
  17. LoPresti, J. Accelerated Service Testing of New and Improved Track Components. 23rd Annual AAR Research Review, Pueblo, CO, USA, 2018.
  18. Kaewunruen, S., E. K. Gamage, and A. M. Remennikov. Modelling Railway Prestressed Concrete Sleepers (Cross-ties) with Holes and Web Openings. *Procedia Engineering*, Vol. 161, 2016, pp. 1240–1246.
  19. Winkler, E. *Theory of Elasticity and Strength*. Prague Dominicus, Czechoslovakia, 1867.
  20. Long, J. Analysis and Design of Deep Foundations, Vol. 2 - Lateral Behavior [unpublished lecture notes]. CEE 585: Deep Foundations, University of Illinois at Urbana-Champaign, 2011.
  21. Kerr, A.D. (IV). Response of Track to Wheel Loads. In: *Fundamentals of Railway Track Engineering*. Omaha, NE, USA: Simmons Boardman, 2003, pp. 84–134.
  22. Federal Highway Administration. Chapter 8. Analyses of the Lateral Load Tests at the Route 351 Bridge. FHWA-HRT 04-043. Federal Highway Administration, Washington, D.C., 2006. <https://www.fhwa.dot.gov/publications/research/infrastructure/structures/04043/08.cfm>. Accessed October 30, 2019.
  23. Hetényi, M. *Beams on Elastic Foundation: Theory with Applications in the Fields of Civil and Mechanical Engineering*. The University of Michigan Press, Ann Arbor, 1946.
  24. Green, D. W., J. E. Winandy, and D. E. Kretschmann. *Mechanical Properties of Wood*. General Technical Report GTR-113. Forest Products Laboratory, USDA Forest Service, Madison, WI, 1999.
  25. Matlock, H. Correlations for Design of Laterally Loaded Piles in Soft Clay. *Proc., 2nd Annual Offshore Technology Conference*, Houston, TX, 1970.
  26. American Railway Engineering and Maintenance-of-Way Association. Chapter 5: Track. In *Manual for Railway Engineering*, The American Railway Engineering and Maintenance-of-Way Association, Landham, MD, 2007.
  27. Gao Y, LoPresti J. Interim Report Broken Spike Remediation. Transportation Technology Center, Inc., Pueblo, CO, USA, 2020, Technology Digest, Report No.: TD-20-004, pp. 4.
  28. Selim, M, M Moore, J Lee, and A Green. *A Sustainable and Durable Glass Reinforced Thermoplastic Composite Railroad Crosstie*. TP19-0831, Granville, Ownes Corning, Science & Technology OH 2019.